



Monitoring Velocity Changes Caused By Underground Coal Mining Using Seismic Noise

RAFAŁ CZARNY,¹ HENRYK MARCAK,¹ NORI NAKATA,² ZENON PILECKI,¹ and ZBIGNIEW ISAKOW³

Abstract—We use passive seismic interferometry to monitor temporal variations of seismic wave velocities at the area of underground coal mining named *Jas-Mos* in Poland. Ambient noise data were recorded continuously for 42 days by two three-component broadband seismometers deployed at the ground surface. The sensors are about 2.8 km apart, and we measure the temporal velocity changes between them using cross-correlation techniques. Using causal and acausal parts of nine-component cross-correlation functions (CCFs) with a stretching technique, we obtain seismic velocity changes in the frequency band between 0.6 and 1.2 Hz. The nine-component CCFs are useful to stabilize estimation of velocity changes. We discover correlation between average velocity changes and seismic events induced by mining. Especially after an event occurred between the stations, the velocity decreased about 0.4 %. Based on this study, we conclude that we can monitor the changes of seismic velocities, which are related to stiffness, effective stress, and other mechanical properties at subsurface, caused by mining activities even with a few stations.

Key words: Monitoring, scattering, coda waves, coal mine, induced seismicity.

1. Introduction

Two techniques of coal exploitation are often used: open-pit mining for shallower coal seams (up to about 300 m) and underground mining for deeper seams. In Poland, underground mining is more common, and people use longwall and room-and-pillar systems for mining. The first one consists of a long wall of coal in a single slice. The latter one refers to

cutting a network of *rooms* into the seam and leaving behind *pillars* to support the roof. Both methods dramatically change stress–strain conditions at and around the mines, and hence the mining changes seismic velocities up to hundreds of meters above the exploitation (HOEK and BROWN 1980; BRADY and BROWN 1993). Dangers of mining especially come from regions of stress concentration, where strong seismicity may be induced (DUBIŃSKI and MUTKE 1996). Therefore, obtaining information on temporal elastic variations near the exploitation area is important. To prevent damages in mine and protect mine crews, some active (DUBIŃSKI and DWORAK 1989; SZREDER *et al.* 2008; HE *et al.* 2011) and passive (ZUBEREK and CHODYN 1989; LURKA 2008; HOSSEINI *et al.* 2012) seismic methods are used to measure elastic moduli. Furthermore, almost all rock burst prone mines in Poland have seismometer networks to observe seismic activity during exploitation. These data are useful for seismic hazard assessment by studying distributions of seismic events (GIBOWICZ and KIJKO 1994; LASOCKI and ORLECKA-SIKORA 2008; LEŚNIAK and ISAKOW 2009). All these methods have one main drawback; these active and passive sources are not temporally continuous because of natural, practical and/or economic reasons. To fill this temporal gap, we use continuous records of ambient seismic noise.

The ambient noise cross-correlation technique (WAPENAAR *et al.* 2010a, b) has been used to monitor temporal velocity changes due to pressure changes in volcanic calderas (SENS-SCHÖNFELDER and WEGLER 2006; BRENGUIER *et al.* 2008a, b), strong earthquakes (WEGLER and SENS-SCHÖNFELDER 2007; BRENGUIER *et al.* 2008a, b; NAKATA and SNIEDER 2012), slow slips (RIVET *et al.* 2011) and landslides (MAINSANT *et al.* 2012). One can also monitor velocities and hence stiffness of civil structures with the ambient noise technique (NAKATA and SNIEDER 2014). According to

¹ The Mineral and Energy Economy Research Institute of the Polish Academy of Sciences, Wybickiego 7, 31-261 Krakow, Poland. E-mail: czarny@min-pan.krakow.pl; marcak@agh.edu.pl; pilecki@min-pan.krakow.pl

² Department of Geophysics, Stanford University, 397 Panama Mall, Stanford, CA 94305, USA. E-mail: nnakata@stanford.edu

³ Institute of Innovative Technologies EMAG, Leopolda 31, 30-189 Katowice, Poland. E-mail: zbigniew.isakow@ibemag.pl

applications, passive seismic interferometry may have different data processing flows. Velocity changes can be estimated from autocorrelation (WEGLER and SENS-SCHÖNFELDER 2007; OHMI *et al.* 2008), cross-correlation (FROMENT *et al.* 2013; HOBIGER *et al.* 2014) or deconvolution (NAKATA and SNIEDER 2012) functions retrieved from ambient seismic noise in variety of temporal resolution.

In this study, we employ ambient noise cross-correlation and stretching techniques to estimate temporal changes in velocities at the coal mine *Jas-Mos* in Poland and to discover their relationship with induced seismicity. We first introduce the setting of the survey at the mine. Next, we show ambient noise characteristic in the area and then explain the method to compute CCFs and to estimate velocity changes with three-component broadband sensors. Finally, we discuss the velocity changes and their relationship with induced seismicity.

2. Survey Setting

The *Jas-Mos* coal mine is located at the south of Poland as one of the six mines in the region (Fig. 1a). On the south side, Poland's mines are bordering on four Czech Republic's mines. All these mines exploit coal with longwall system. The seismicity activities at *Jas-Mos* are not very high and the energy of seismic events has rarely exceeded 10^6 J ($M = 2.4$). The energy expressed in Joule (E) is linked with Richter magnitude (M) by empirical formula (DUBINSKI and WIERZCHOWSKA 1973):

$$\log E = 1.97 + 1.7M \quad (1)$$

We deployed two broadband three-component seismometer stations (Guralp CMG-6TD: stations s1 and s2 in Fig. 1) at the surface around coal longwalls in zones C3, W3 and ZM (Fig. 1b, blue polygons). The data were sampled with 0.01 s. The distance between these stations was 2.8 km. These longwalls as well as longwalls from surrounding mines were exploited during 42 days of seismic noise recording from 2 August 2013 to 12 September 2013. The thicknesses of mined seams in *Jas-Mos* are about 3.5 m, and the depths are about 600 m at zone ZM and 800 m at zones C3 and W3.

Two geological cross-sections close to the survey area are shown in the Fig. 2. The exploited rock mass (Upper Carboniferous), strongly disturbed by faults, is mostly composed by clastic rocks, such as: sandstones, siltstones, mudstones and claystones with coal seams (Namurian-Westphalian), referred to as the productive coal measures. The Upper Carboniferous rocks are covered by Miocene and Quaternary sediments. The Miocene and Quaternary materials consist of gravels, sands, clay, claystones, etc. Beneath the exploited Upper Carboniferous sediments, the Lower Carboniferous rocks exist, referred as the Culm facies in that region. The Carboniferous deposits are dipping gently from south to north. The Carboniferous deposits are on top of a crystalline basement, at variable depths from 1800 m and more gaining 3500 m.

3. Seismic Noise in Area

Because the natural seismic activities around the survey area are low and the area is far from ocean, the main sources of ambient noise are urban activity and mining, especially at high frequencies. Mining generates three types of noise sources: noise associated with overburden subsidence, from exploitation machineries and from induced seismicity. Therefore, spectral content and direction of the seismic noise are connected with intensity of exploitation and its position. Differences in the amplitude spectra and spatial distribution of seismic noise can cause biases in estimation of seismic velocity (HADZIOANNOU *et al.* 2009; ZHAN *et al.* 2013). Because we have only two sensors, directional analyses are difficult, but fortunately, mining activities surround the sensors, and activity level does not vary during the acquisition compared with our time windows as explained below.

Power spectral density (PSD) curves for each day over the week of August 5 for station s1 (Fig. 3a–c) show that the energy of the noise on the weekdays (red curves) is stable in the frequency of range 0.6–10 Hz. On the weekend, PSD (black curves) in this frequency range is much smaller. Due to the lack of exploitation at mines and smaller traffic at the urban area at weekends, we conclude that the seismic energy in this frequency range is mainly related to

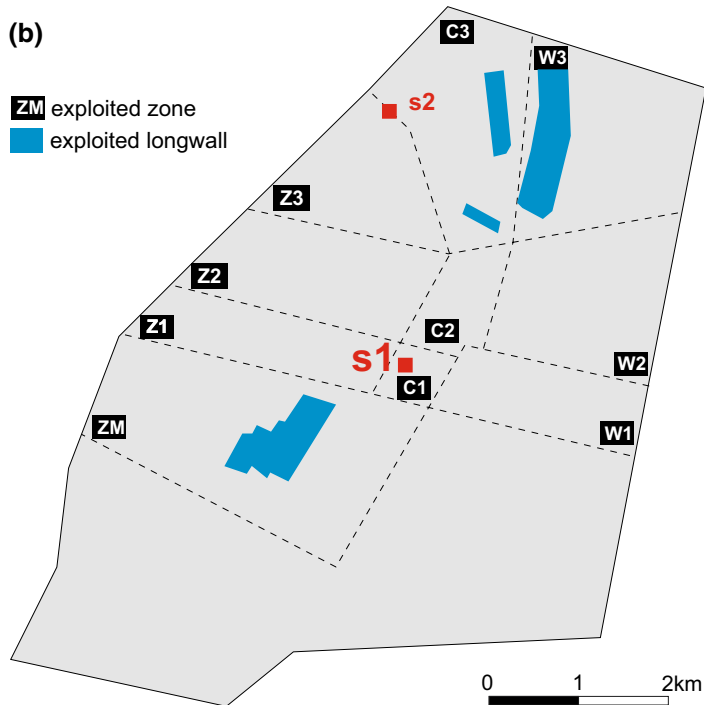
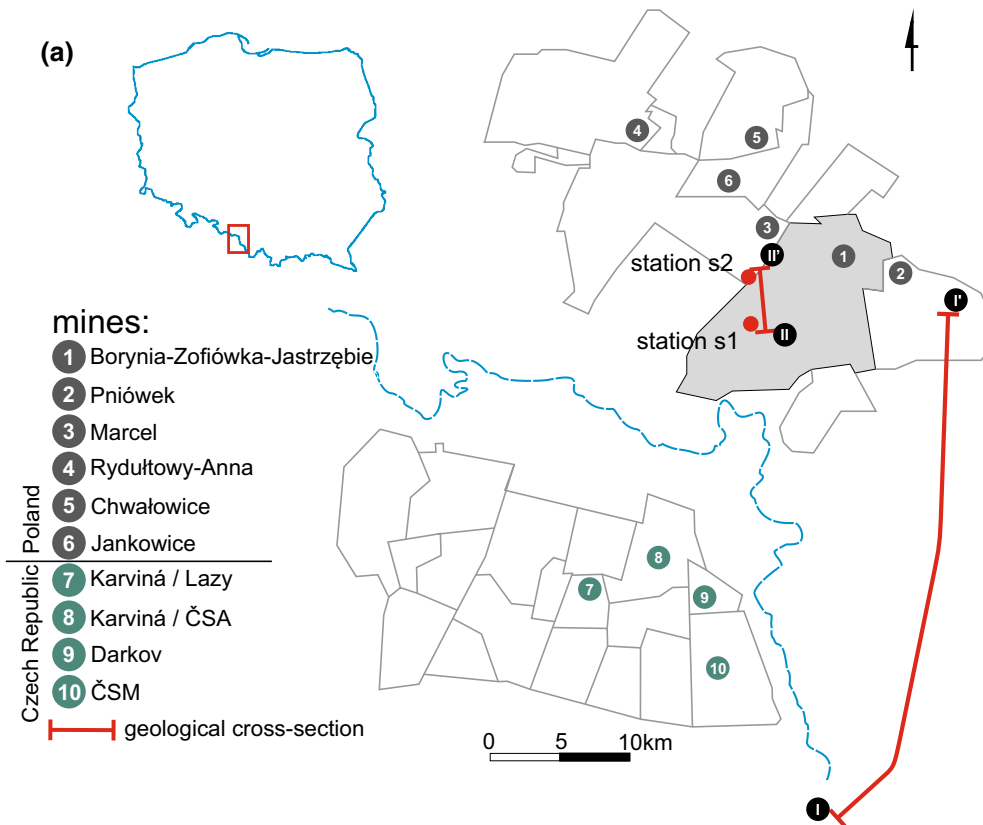


Figure 1

a Locations of mines in Poland (from 1 to 6) and Czech Republic (from 7 to 10), seismometers *s1* and *s2*, and two geological cross-sections I–I' and II–II' shown in Fig. 2. **b** The mine area with exploitation zones. Blue polygons are exploited longwalls in zone ZM, C3 and W3 during the data acquisition

mining activities. For monitoring seismic velocity changes, we focus on the frequency band between 0.6 and 1.2 Hz, which roughly corresponds to the sensitivity depth of 500–1000 m where the mine seams exist. To calculate this depth range, we assume that surface waves dominate in seismic noise wavefields at the frequency range considered and the average shear wave velocity for Upper Carboniferous in the region is about 2200 m/s (BAIA and WITEK 2007). Seismic noise at frequency higher than 1.2 Hz is sensitive to soft sediment layer up to 200 m depth (Fig. 2b).

For better understanding of the temporal variation of spectral content of ambient noise energy in the selected frequency band, we analyze the hourly PSD variation averaged over three components of station *s1* and 3 components of station *s2* as $\frac{\sum_{c=1}^6 \int_{f_1}^{f_2} PSD df}{6}$, where f_1 and f_2 define our target frequency range (here, 0.6 and 1.2 Hz, respectively) (Fig. 3e). Averaged PSD has a daily cycle due to urban activities and daily exploitation schedule. At weekends and holiday

on 15 August 2013 (the gray shade in Fig. 3e), the exploitation is stopped and the energy of ground motion is small.

Induced seismicity was also observed around the mining zones (Fig. 3d, f). During the 42 days of seismic noise measurement, Jas-Mos mine seismic network recorded 1500 events. Over 700 of them had energy higher than 10^3 J. Although seismic noise sources generated by mining longwalls in zones ZM, C3, W3 (Fig. 3d, boxes filled by straight lines) were out of the stationary phase for correlation analyses, their positions were stable over the measurements because exploitation was implemented at the same areas continuously. Activities of other mines are also contributing to extract the wave propagation with cross-correlation because the mines surround the stations (Fig. 1).

4. Data Processing

4.1. Computation of Cross-Correlation Functions

To monitor small velocity changes caused by coal mining, we follow a technique proposed by HOBIGER *et al.* (2012). They computed CCFs for all component combinations and averaged the estimated velocity changes over all combinations to increase the stability and reduce biases caused by irregular noise

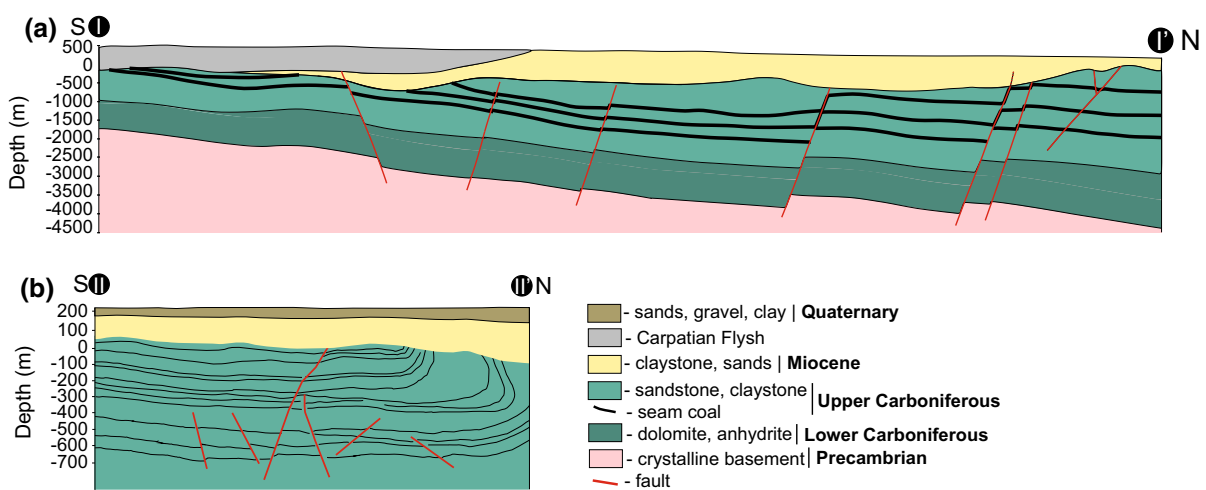


Figure 2

Geological cross-sections along the profiles I–I' and II–II' in Fig. 1: **a** across Poland's and Czech Republic's mines and **b** nearby stations *s1* and *s2*

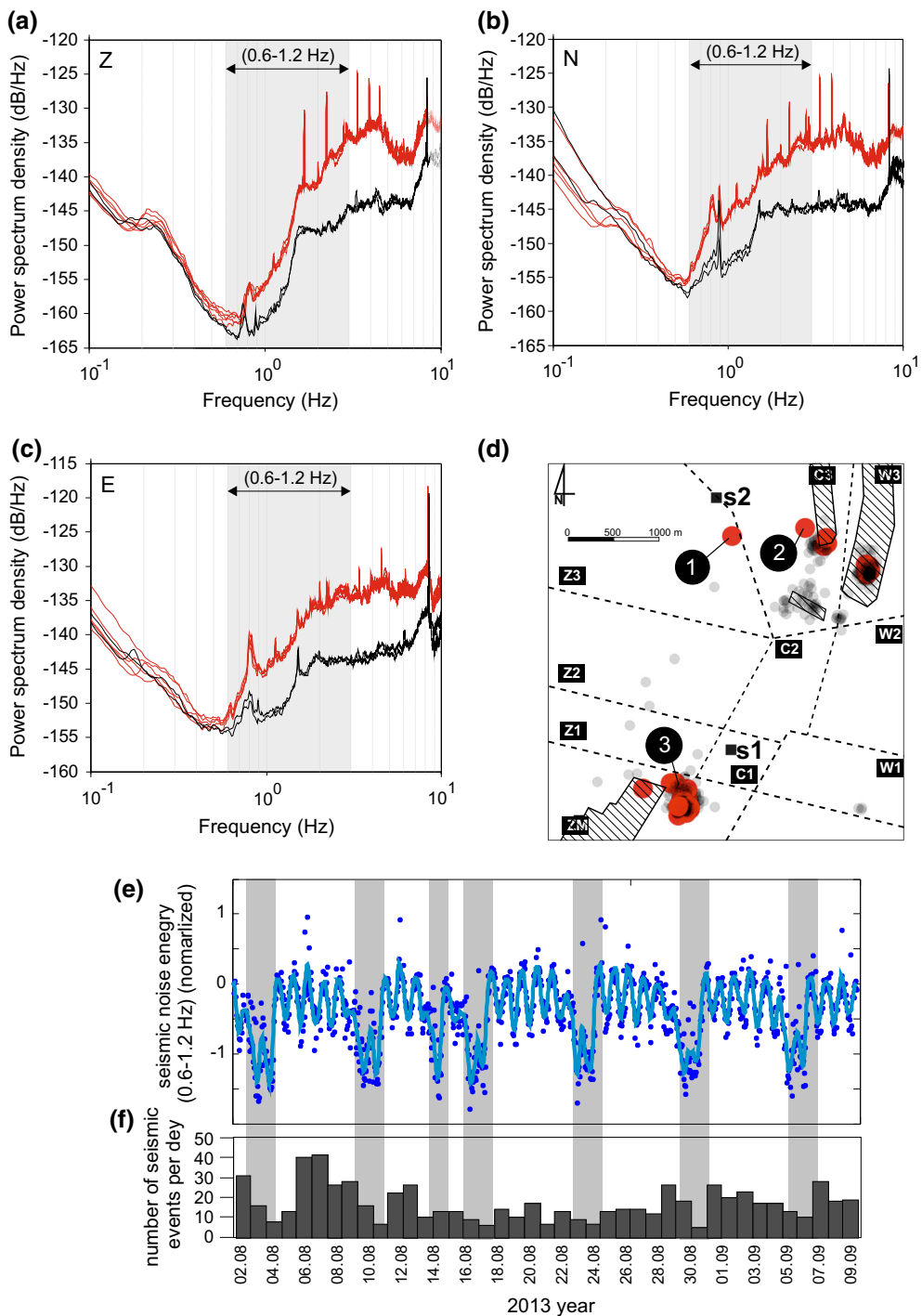


Figure 3

Power spectrum density curves estimated from ambient noise data for **a** vertical and **b**, **c** two horizontal components at station *s1*. The red curves are computed for days with coal exploitation and the black curves without. **d** Epicenters of seismic events (higher than 10^4 J—red dots; higher than 10^3 J—gray dots) together with mining longwalls (polygons filled with straight lines). Events labeled by 1–3 are discussed in Sect. 5. **e** Hourly power spectrum density in frequency band 0.6–1.2 Hz averaged over all components of two stations. Gray boxes indicate days without exploitation (weekends and holidays). **f** The number of induced seismic events per day at the mine

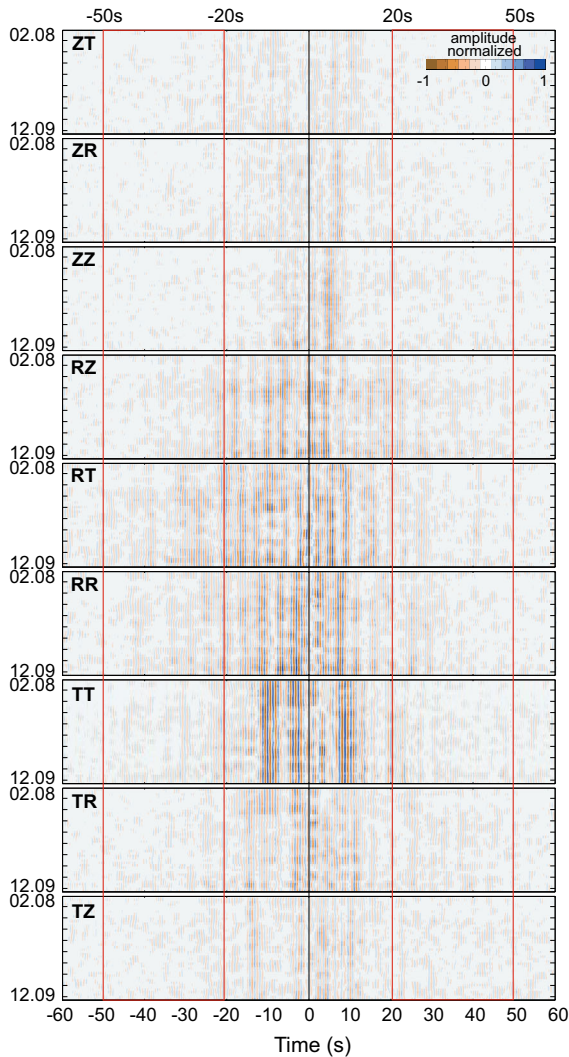


Figure 4

Causal and acausal parts of cross-correlation functions up to \pm first 60 s for all combinations of components. The *red rectangles* show the time windows we used for estimation of velocity changes. Normalization is common to all components and relative amplitudes are preserved

distribution. To further improve the accuracy of the velocity measurement, we use only coda parts of CCFs for the estimation. Because the coda waves scatter multiple times, the waves sample larger areas than ballistic waves and are less sensitive for noise sources distribution.

To compute CCFs, we employ the noise-correlation processing of BENSEN *et al.* (2007), which contains spectral whitening between 0.6 and 1.2 Hz and one-bit normalization. To improve the signal-to-

noise ratio of CCFs, we use a moving average in three-day window. Figure 4 shows the CCFs for all combinations of components. The stations are aligned nearly north–south direction, and hence we assume that the north and east components recorded radial and transversal ground motions, respectively. Hereafter, we indicate vertical, radial and transverse components by Z, R and T letters, respectively. Combination of letters such as TZ means cross-correlation functions between T component at station s1 and Z component at station s2. Based on calculation of cross-correlation, station s1 behaves as a virtual source (i.e., waves in the causal part of CCFs propagate from s1 to s2).

The three-day CCFs are highly similar each other during the entire time interval (Fig. 4). Note that even in the time interval of coda waves (the red rectangles), the waves are coherent among different dates, which is important for estimating accurate velocity changes using the stretching technique. TT component shows the strongest amplitudes in the ballistic part (1–10 s), which means we retrieve strong Love waves, although the coda waves in TT component is not strong. The symmetry of waves in the causal and acausal parts is not satisfied well especially for component pairs which contain Z. This is because of uneven noise distribution and probably due to geological structure in the mine region. We can weaken this effect by averaging over the causal and acausal information during the velocity estimation.

4.2. Estimation of Velocity Changes From Coda Waves

We compare each three-day CCF with the reference traces, which are the averaged waveforms over all CCFs at each combination of components. We analyze time windows from ± 20 to 50 s associated with coda waves (the red rectangles in Fig. 4). To measure the relative velocities according to the reference traces, we use a stretching technique (HADZIOANNOU *et al.* 2009):

$$CC(\varepsilon) = \frac{\int f_{\text{imp}}(t(1-\varepsilon))f_{\text{ref}}(t)dt}{\sqrt{\int (f_{\text{imp}}(t(1-\varepsilon)))^2 dt \int (f_{\text{ref}}(t))^2 dt}}, \quad (2)$$

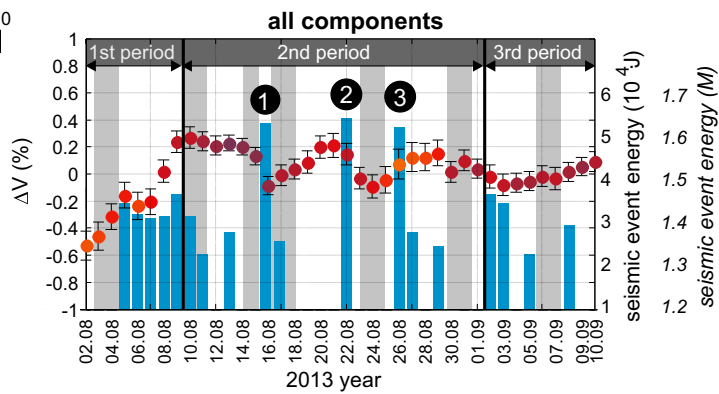
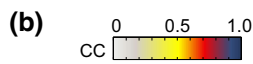
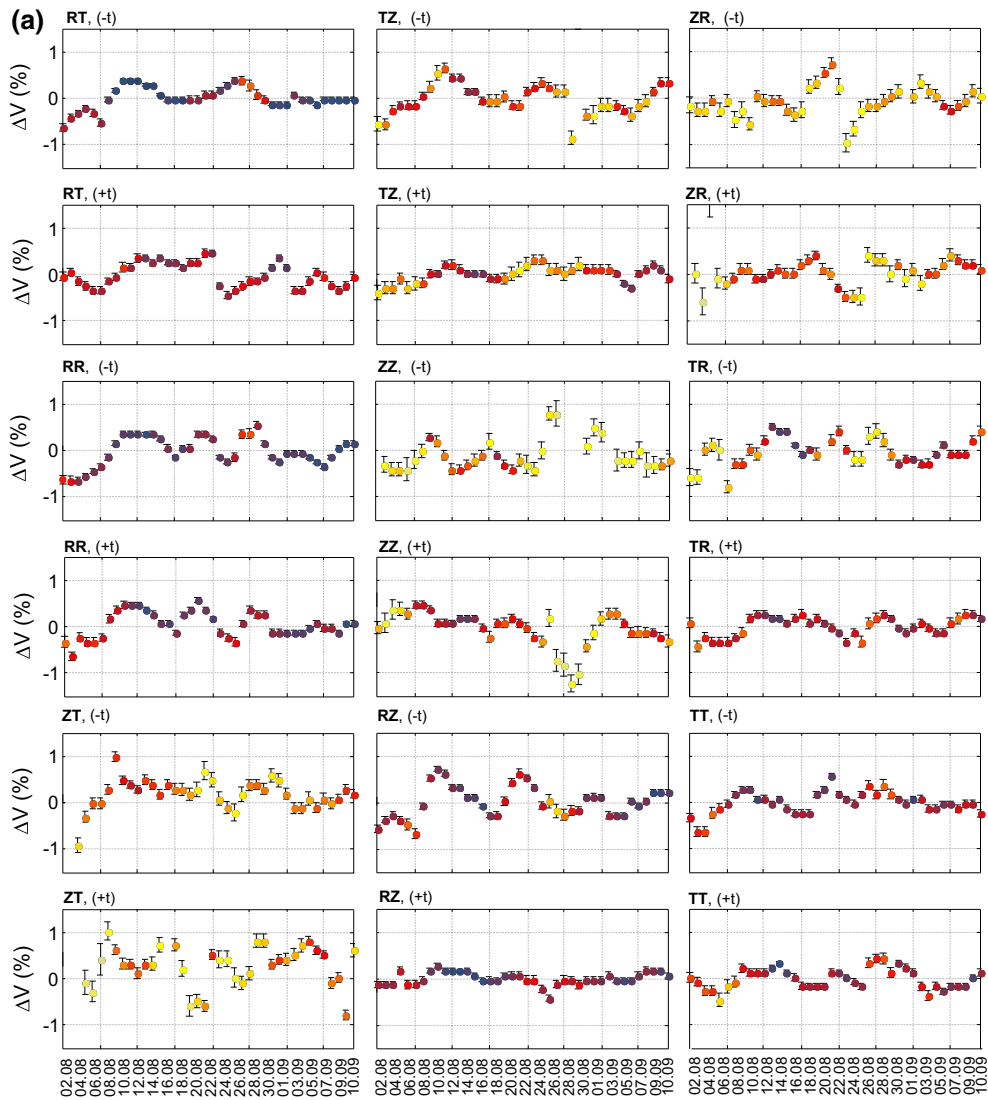


Figure 5

a Temporal velocity perturbations estimated for coda wave (for time windows from $-/+20$ to 50 s in positive and negative times) for all component combinations in conjunction with errors calculated by Eq. 6. The positive ΔV means the velocity faster than the reference velocity. b Relative velocity changes of coda wave (dots) with reference to the energy of main seismic events (blue bars). Days with gray background are free of exploitation.

Colorbar is common for (a, b)

where ε is a stretching parameter, f_{tmp} represents temporal (three-day averaged) CCFs, and f_{ref} describes reference trace. Note that the CCFs are time windowed to focus on the coda part.

The stretching parameter (ε) for the maximum value of CC corresponds to velocity changes between reference trace and trace of the day:

$$\varepsilon = \frac{\Delta V}{V}, \quad (3)$$

where V is the velocity for the reference trace and ΔV is velocity difference at each temporal CCF compared with the reference trace. Figure 5 presents the obtained temporal velocity perturbation curves in 18 different combinations (9 components both causal and acausal). Velocity changes for the causal part of CCFs have higher correlation coefficients than the acausal part, which is probably because we have better illumination of noise sources from Czech Republic's mines (Fig. 1). There are also noticeable differences in the range of velocity changes between each component combination. Velocities with component Z have the largest variations. These changes have very weak correlation coefficients and might be artifacts due to the influence of underground mining tremors. By following HOBIGER et al. (2012), we reduce this effect by estimating average velocity changes $\Delta V_a(\tau)$ and average correlation coefficient $CC_a(\tau)$ using the expressions of

$$\Delta V_a(\tau) = \frac{\sum_{k=1}^N CC_k^2(\tau) \cdot \Delta V_k(\tau)}{\sum_{k=1}^N CC_k^2(\tau)}, \quad (4)$$

$$CC_a(\tau) = \frac{\sum_{k=1}^N CC_k^3(\tau)}{\sum_{k=1}^N CC_k^2(\tau)}, \quad (5)$$

where N is the number of component combinations for causal and acausal parts and equals to 18 and τ is a measurement day. Figure 5b shows the averaged velocity changes and correlation coefficients.

To validate the velocity changes, we estimate root mean square error of the changes (WEAVER et al. 2011):

$$\text{RMS}_{\text{error}} = \frac{\sqrt{1 - \text{CC}^2}}{2\text{CC}} \sqrt{\frac{6\sqrt{\frac{\pi}{2}}T}{\omega_c^2(t_2^3 - t_1^3)}}, \quad (6)$$

where T is the width of used wave periods, t_1 and t_2 are the start and end time of the time-window, respectively, and ω_c is the central frequency of analyzed seismic wave. $\text{RMS}_{\text{error}}$ informs whether velocity changes are due to sources or due to medium changes. The errors are small enough to accurately estimate daily velocity changes (Fig. 5a, b).

4.3. Discussion of Velocity Changes Estimated By Coda Wave Interferometry

In the Fig. 5b, we show the estimated average seismic velocity changes from the coda waves and the total seismic energy for events stronger than 10^4 J ($M = 1.2$) per day. For interpretation, we divide the velocity changes into three groups: from August 2 to August 9, from August 10 to September 1, and from September 2 to September 10.

In the first period, the velocity is lower with respect to the reference CCF trace at the beginning and gradually increases with date. Although we do not have a clear conclusion about this behavior of the velocities yet, we speculate that the ZM zone is key to understand this velocity change. During this time interval, the area ZM is very active, and most of seismic events are related to this area. As we explain later, when the area ZM is active, the velocities between two stations apparently increase. To study this phenomenon, we need more detail wavefields sampling (i.e., denser station coverages).

In the second period, we have three relatively large events (Events 1, 2 and 3; Fig. 3d). Event 1 is the closest one to the direct path between the stations, and we observe the clear reduction of the velocity. Event 2 is not on the direct path, but because we use coda waves, and mines are highly scattering media, we still observe some decrease in the velocity. Note that each dot in Fig. 5b shows the three-day average relative velocities, and depending on the origin time of the event, the velocity changes on the event day or the next day. Although Event 3 is also large, the

location of the potential damage area around the epicenter may not be sampled well by coda waves. Hence, we find almost no changes on average velocity change curve (Fig. 5b). Using these receivers, we can monitor the velocity changes in the area (including the area of Event 2, but not Event 3). Interestingly, the velocity slightly increases around the date of Event 3. This might be because the healing after Event 2. We also speculate that this could be caused by the event (Event 3) in area ZM as similar to the first period.

In the third period we do not observe considerable velocity changes. It is probably because of all intermediate-size events have epicenters in W3 zone (Fig. 3d).

5. Conclusions

We discover seismic velocity changes during underground coal mining using passive seismic interferometry with two seismometers. The multicomponent analysis helps to stabilize the estimated velocity changes. The seismic velocities decrease when a large event occurred close to the direct wave path between two receivers used. Because we use coda waves, the sensitivity of the velocity changes is larger than just on the direct path of stations. The sensitivity relates to the receiver location, noise environment, and local geology. In this study, we show a potential to use a few sensors to monitor the seismic activities and the ground response of them. To understand the response of the events that are far from the stations, we need to deploy more sensors; therefore, the sensor location is important for the monitoring.

Acknowledgments

This article was prepared as a result of the LOFRES Project No PBS1/A2/13/2013 performed within the 1st call of the Applied Research Programme co-financed by the National Centre for Research and Development in Poland. We thank the editor and two anonymous reviewers for valuable comments and discussions.

REFERENCES

- BAIA, M., and K. WITEK (2007), *Model prędkościowy fal P i S oraz gęstości objętościowych dla wybranych otworów w rejonie Karpat Zachodnich*, Geol. i Akad. Górniczo-Hutnicza im. Stanisława Staszica w Krakowie, 33(4/1), 59–80 (In Polish).
- BENSEN, G. D., M. H. RITZWOLLER, M. P. BARMIN, A. L. LEVSHIN, F. LIN, M. P. MOSCHETTI, N. M. SHAPIRO, and Y. YANG (2007), *Processing seismic ambient noise data to obtain reliable broadband surface wave dispersion measurements*, Geophys. J. Int., 169, 1239–1260, doi:10.1111/j.1365-246X.2007.03374.x.
- BRADY, B. H. G., and E. T. BROWN (1993), *Rock mechanics: for underground mining*, Chapman & Hall.
- BRENGUIER, F., M. CAMPILLO, C. HADZIOANNOU, N. M. SHAPIRO, R. M. NADEAU, and E. LAROSE (2008a), *Postseismic relaxation along the San Andreas fault at Parkfield from continuous seismological observation.*, Science, 321(5895), 1478–81, doi:10.1126/science.1160943.
- BRENGUIER, F., N. M. SHAPIRO, M. CAMPILLO, V. FERRAZZINI, Z. DUPUTEL, O. COUTANT, and A. NERCESSIAN (2008b), *Towards forecasting volcanic eruptions using seismic noise*, Nat. Geosci., 1(2), 126–130, doi:10.1038/ngeo104.
- DUBIŃSKI, J., and Z. WIERZCHOWSKA (1973), *Methods of calculation of seismic energy for mining tremors (in Polish)*, Pr. GIG, Komun. GIG, 591.(In Polish).
- DUBIŃSKI, J., and J. DWORAK (1989), *Recognition of the zones of seismic hazard in Polish Coal mines by using a seismic method*, Pure Appl. Geophys., 129(3–4), 609–617, doi:10.1007/BF00874528.
- DUBIŃSKI, J., and G. MUTKE (1996), *Characteristics of mining tremors within the near-wave field zone*, Pure Appl. Geophys., 147(2), 249–261, doi:10.1007/BF00877481.
- FROMENT, B., M. CAMPILLO, J. H. CHEN, and Q. Y. LIU (2013), *Deformation at depth associated with the 12 May 2008 MW 7.9 Wenchuan earthquake from seismic ambient noise monitoring*, Geophys. Res. Lett., 40(11–2012), 78–82, doi:10.1029/2012GL053995.
- GIBOWICZ, S., and A. KIJKO (1994), *An introduction to mining seismology*, Academic Press, New York.
- HADZIOANNOU, C., E. LAROSE, O. COUTANT, P. ROUX, and M. CAMPILLO (2009), *Stability of monitoring weak changes in multiply scattering media with ambient noise correlation: laboratory experiments.*, J. Acoust. Soc. Am., 125, 3688–3695, doi:10.1121/1.3125345.
- HE, H., L. DOU, X. LI, Q. QIAO, T. CHEN, and S. GONG (2011), *Active velocity tomography for assessing rock burst hazards in a kilometer deep mine*, Min. Sci. Technol., 21(5), 673–676, doi:10.1016/j.mstc.2011.10.003.
- HOBIGER, M., U. WEGLER, K. SHIOMI, and H. NAKAHARA (2012), *Coseismic and postseismic elastic wave velocity variations caused by the 2008 Iwate-Miyagi Nairiku earthquake, Japan*, J. Geophys. Res., 117(B9), B09313, doi:10.1029/2012JB009402.
- HOBIGER, M., U. WEGLER, K. SHIOMI, and H. NAKAHARA (2014), *Single-station cross-correlation analysis of ambient seismic noise: application to stations in the surroundings of the 2008 Iwate-Miyagi Nairiku earthquake*, Geophys. J. Int., 198(1), 90–109, doi:10.1093/gji/ggu115.
- HOEK, E., and E. T. BROWN (1980), *Underground excavations in rock*, Institution of Mining and Metallurgy, London.

- HOSSEINI, N., K. ORAEE, K. SHAHRIAR, and K. GOSHTASBI (2012), *Passive seismic velocity tomography on longwall mining panel based on simultaneous iterative reconstructive technique (SIRT)*, *J. Cent. South Univ.*, 19(8), 2297–2306, doi:[10.1007/s11771-012-1275-z](https://doi.org/10.1007/s11771-012-1275-z).
- LASOCKI, S., and B. ORLECKA-SIKORA (2008), *Seismic hazard assessment under complex source size distribution of mining-induced seismicity*, *Tectonophysics*, 456(1–2), 28–37, doi:[10.1016/j.tecto.2006.08.013](https://doi.org/10.1016/j.tecto.2006.08.013).
- LEŚNIAK, A., and Z. ISAKOW (2009), *Space–time clustering of seismic events and hazard assessment in the Zabrze-Bielszowice coal mine, Poland*, *Int. J. Rock Mech. Min. Sci.*, 46(5), 918–928, doi:[10.1016/j.ijrmms.2008.12.003](https://doi.org/10.1016/j.ijrmms.2008.12.003).
- LURKA, A. (2008), *Location of high seismic activity zones and seismic hazard assessment in Zabrze Bielszowice coal mine using passive tomography*, *J. China Univ. Min. Technol.*, 18(2), 177–181, doi:[10.1016/S1006-1266\(08\)60038-3](https://doi.org/10.1016/S1006-1266(08)60038-3).
- MAINSANT, G., E. LAROSE, C. BRÖNNIMANN, D. JONGMANS, C. MICHOD, and M. JABOYEDOFF (2012), *Ambient seismic noise monitoring of a clay landslide: Toward failure prediction*, *J. Geophys. Res.*, 117(F1), F01030, doi:[10.1029/2011JF002159](https://doi.org/10.1029/2011JF002159).
- NAKATA, N., and R. SNIEDER (2012), *Time-lapse change in anisotropy in Japan's near surface after the 2011 Tohoku-Oki earthquake*, *Geophys. Res. Lett.*, 39(11), doi:[10.1029/2012GL051979](https://doi.org/10.1029/2012GL051979).
- NAKATA, N., and R. SNIEDER (2014), *Monitoring a building using deconvolution interferometry. II: ambient-vibration analysis*, *Bull. Seismol. Soc. Am.*, 104, 204–213, doi:[10.1785/0120130050](https://doi.org/10.1785/0120130050).
- OHMI, S., K. HIRAHARA, H. WADA, and K. ITO (2008), *Temporal variations of crustal structure in the source region of the 2007 Noto Hanto Earthquake, central Japan, with passive image interferometry*, *Earth, Planets Sp.*, 60(10), 1069–1074, doi:[10.1186/BF03352871](https://doi.org/10.1186/BF03352871).
- RIVET, D., M. CAMPILLO, N. M. SHAPIRO, V. CRUZ-ATIENZA, M. RADIGUET, N. COTTE, and V. KOSTOGLODOV (2011), *Seismic evidence of nonlinear crustal deformation during a large slow slip event in Mexico*, *Geophys. Res. Lett.*, 38(8), doi:[10.1029/2011GL047151](https://doi.org/10.1029/2011GL047151).
- SENS-SCHÖNFELDER, C., and U. WEGLER (2006), *Passive image interferometry and seasonal variations of seismic velocities at Merapi Volcano, Indonesia*, *Geophys. Res. Lett.*, 33(21), L21302, doi:[10.1029/2006GL027797](https://doi.org/10.1029/2006GL027797).
- SZREDER, Z., Z. PILECKI, and J. KLOSINSKI (2008), *Effectiveness of recognition of exploitation edge influence with the help of profiling of attenuation and velocity of seismic wave*, *Gospod. SUROWCAMI Miner.*, 24, 215–226.
- WAPENAAR, K., D. DRAGANOV, and R. SNIEDER (2010a), *Tutorial on seismic interferometry: Part 1—Basic principles and applications*, *Geophysics*, 75, 75A195–75A209, doi:[10.1190/1.3457445](https://doi.org/10.1190/1.3457445).
- WAPENAAR, K., E. SLOB, R. SNIEDER, and A. CURTIS (2010b), *Tutorial on seismic interferometry: Part 2—Underlying theory and new advances*, *Geophysics*, 75, 75A211, doi:[10.1190/1.3463440](https://doi.org/10.1190/1.3463440).
- WEAVER, R. L., C. HADZIOANNOU, E. LAROSE, and M. CAMPILLO (2011), *On the precision of noise correlation interferometry*, *Geophys. J. Int.*, 185, 1384–1392, doi:[10.1111/j.1365-246X.2011.05015.x](https://doi.org/10.1111/j.1365-246X.2011.05015.x).
- WEGLER, U., and C. SENS-SCHÖNFELDER (2007), *Fault zone monitoring with passive image interferometry*, *Geophys. J. Int.*, 168, 1029–1033, doi:[10.1111/j.1365-246X.2006.03284.x](https://doi.org/10.1111/j.1365-246X.2006.03284.x).
- ZHAN, Z., V. C. TSAI, and R. W. CLAYTON (2013), *Spurious velocity changes caused by temporal variations in ambient noise frequency content*, *Geophys. J. Int.*, 194(3), 1574–1581, doi:[10.1093/gji/ggt170](https://doi.org/10.1093/gji/ggt170).
- ZUBEREK, W., and L. CHODYN (1989), *Practical application of the phenomenon of acoustic emission in rock*, *Arch. Acoust.*, 14, 123–142.

(Received August 14, 2015, revised December 17, 2015, accepted December 23, 2015, Published online January 14, 2016)